Molecular Mobility in Wool Fibers as Determined from Nuclear Magnetic Resonance Studies

D. RAMA RAO* and V. B. GUPTA

Cotton Technological Research Laboratory, Matunga, Bombay-400019, and Department of Textile Technology, Indian Institute of Technology, Hauz khas, New Delhi 110016, India

SYNOPSIS

The mobility of protons in wool samples of Lincoln, Chokla, and Merino, equilibrated to various moisture contents in the range of 0–98% relative humidity (RH), have been studied by pulsed nuclear magnetic resonance (NMR) technique. Peak height and peak width were determined from absorption and derivative curves and the relaxation times T_1 and T_2 were determined from relaxation curves. The mobility increases with increase in moisture content. Among the three wools, the mobility was high in Merino as compared to the other two wools. The differences in the measured mobilities were related to structural and morphological differences in the three wools. The present analysis suggests that water in wool has at least three different associations, each with a different binding energy.

INTRODUCTION

Nuclear magnetic resonance (NMR) method is perhaps one of the most suitable for obtaining direct information on the various molecular motion processes involved, and it has been extensively used for the study of multiple transitions, crosslinking processes, and aging and environmental effects in polymers.[1] In the case of wool fibers proton resonance line shapes and relaxation times have been reported as a function of moisture content;[2-9] in every case the relatively narrow signal from the sorbed water could be distinguished from the broad resonance of the substrate. The width of the resonance decreased with increase in moisture content as a result of the increasing mobility of the sorbed water. West et al.[9] showed that the mobility of water in wool increases considerably as the relative humidity (RH) increases from 25 to 80%, but the rate of increase of mobility with moisture regain is less at higher humidities. They also found that all water protons in wool are less firmly bound than the keratin protons but less mobile than liquid water. Svanson[8] has shown that water is present in two main states of different mobilities and that the overlap between the signal contributions from water with reduced mobility and from the polymer chains makes observations of the segmental mobility of the polymer chains difficult. Olf and Peterlin[10] studied nylon 66 fiber and reported that a sharp line due to mobile water molecules appears at water regains of 1.4% and higher, and the amount of mobile water was always found to be smaller than the amount of water absorbed. A mobile polymer line appears at water contents close to saturation with a width intermediate between the broad line and the sharp water line. A similar observation was reported by Miyagawa et al.[5] for wool, silk, and nylon fibers.

Decay of magnetization using pulsed NMR methods have been widely used to study the state of water in various hydrophilic materials. Lynch and Marsden[4] conducted a study of wool–water system, and their studies suggest that the variable slow decaying component, which was attributed to the protons of the absorbed water, showed different relaxation rates. The model for the wool–water system proposed by Feughelman and Haly[11] was found to explain their results reasonably well.

Wools of different biological origin are known to show differences in their properties that, in turn, were related to differences in structure and morphology. However, there is hardly any reported study on the changes in molecular mobility as related to such differences. In the present studies the pulsed

* To whom correspondence should be addressed.

Journal of Applied Polymer Science, Vol. 44, 623–632 (1992)
 CCC 0021-8995/92/040623-10$04.00

NMR technique was used to characterize Merino, Chokla, and Lincoln wool fibers containing different amounts of moisture with particular emphasis on the characterisation of their molecular mobility.

EXPERIMENTAL

Sample Preparation

Lincoln, Chokla, and Merino wool fibers, properly cleaned, washed, and dried, were cut with the help of scissors into small pieces with powderlike consistency. A 100-mg powder sample was placed in 5-mm internal diameter NMR glass tubes. The sample rose to a height of 15 mm in the tube; since this was less than the height of the specimen coils, no compression of the powder was necessary. The samples in the NMR tubes were hydrated by equilibrating over appropriate saturated salt solutions,[12] in the range 0 to 98% RH, for about 4 weeks before the test. Samples with moisture regains of 0, 10.3, 13.8, 20, and 30% were thus prepared and studied.

Some melted samples were also prepared by heating the fibers for about 60 min in water at 135°C in free condition and at 125°C in stretched (40%) condition. NMR studies on these samples were carried out in the conditioned atmosphere of the laboratory, i.e., at 40 ± 5% RH and 20 ± 1°C.

NMR MEASUREMENTS

The Spectrometer

NMR signals and proton relaxation times were obtained using a Bruker CSP-300 pulsed FT-NMR spectrometer operating at 300 MHz. The spectrometer was equipped with a computer data system. In all the studies pulses of 10 μs width were used, and the data was collected and stored at 1-μs interval.

Spin–Spin Relaxation Time (T_2)

As solid keratin has low T_2 (of the order of 10 μs), the loss of signal due to the pulse width and receiver dead time were minimized by examining induction signal in the form of solid echo using quadrupolar echo pulse sequence given by 90° − t − 180° − AQ − RD, where AQ, the acquisition time was 0.2 s, RD, the recycle time was 2 s, and pulse width and pulse separation (t) were 10 μs. The RF field was swept over 500 kHz (sweep width) and the data was accumulated over 50 scans. All the hydrated samples were scanned under the same identical conditions.

The decay of signal following echo maxima can be expressed as

$$M(t) = \sum_i M_i \exp\left(-\frac{t}{T_{2i}}\right) \qquad (1)$$

where T_{2i} is the spin–spin relaxation time of the ith component, $M(t)$ is total signal intensity at time t and M_i is intensity of ith component and is proportional to number of segments in this component.

Absorption and Derivative Curves

Since the signal following the echo maximum is a Fourier transform of the line shape of the absorption envelope, the absorption curves were obtained using pulse sequence essentially similar to the one described here except for the signal detection mode. In the present case the signal was recorded with quadrature on mode such that echo maximum corresponds to central maxima of the absorption line. The spectrometer, when operated under these conditions, gave a line width of 15 Hz for wool sample with excess water, which was at least 50 times the line width of the narrow line of hydrated wool sample.

Spin–Lattice Relaxation Time (T_1)

T_1 was measured by inversion recovery Fourier transform (IRFT) method employing a pulse sequence of 180° − t − 90° − AQ − RD with AQ + RD > $5T_1$; the acquisition time being 2 μs and the recycle delay being 10 s. T_1 was calculated by null method,[13] in which t was varied until the amplitude of the signal was reduced to zero. T_1 was measured with an accuracy of 5%.

Magic Angle Spinning (MAS)

Proton MAS was measured on samples of Chokla wool conditioned at 10.3% moisture regain (in the ambient atmosphere). Samples were taken in 7-mm zirconium rotor and CP-MAS spectra was observed on proton decoupler channel under low power conditions.[14] The 90° pulse was typically 5 μ s and quadrature phase cycling was used to minimize spectral artifacts.

Mobility Factor

Mobility factor, which is defined as peak height per unit regain,[9] was measured from the peak heights

of the narrow line in wool–water systems. This parameter is a function of both quantity and mobility of water protons and will be expected to reflect the mobility of water protons in the wool–water systems.

RESULTS AND DISCUSSION

Typical Resonance Curve from Hydrated Wool Sample

In the present studies the broad line absorption and derivative curves were obtained by Fourier transformation of the time-dependent decay of intensity to frequency domain and the line width, peak height (maximum intensity), and the area under the curve were measured directly. As an illustration, Figure 1(a) and 1(b) shows the absorption and first derivative curves for Chokla wool sample equilibrated at 10.3% regain. The narrow line is due to protons of the absorbed water, and this is superimposed on the broad line, which is so small in amplitude that it becomes indistinguishable from the general noise in the apparatus and which arises from the protons of the wool keratin. The line width of the broad component is about 27 kHz while that of the narrow line is about 1 kHz. In the pulsed NMR technique both the signals are simultaneously recorded.

These results were obtained with the sample tube spinning perpendicularly to the static field direction at 20 Hz. For MAS the sample was spun at the magic angle of 54.7° to the field direction at frequencies between 1000 and 4200 Hz; the resonance lines obtained show progressive reduction of the line width with increase in frequency of sample spinning (Fig. 2). This reduction of the line width is due to better averaging of local field, thereby reducing the observed line width.

For the work on hydrated wools MAS was not used due to experimental difficulties in obtaining hydrated wool samples. However, the line width obtained from MAS was found to be comparable to the line width obtained from T_2 (shown later) as the pulse technique also minimizes the effect of inhomogeneous broadening on the line width.

Influence of Moisture on NMR Signals

The resonance curves for Chokla wool powder samples equilibrated at 0, 10.3, 13.8, 20, and 30% regain are shown in Figure 3. The data for the other two wools also show similar features. In plotting the absorption data for the three wools studied, the highest intensity was obtained for Merino wool at 30% regain, and this was taken as unity; the intensities obtained for other samples were appropriately scaled by the data processing unit. Since pure water tested under identical conditions gives a narrow line (ca. 15 Hz) of much higher intensity, the present data shows that water protons in wool show much less mobility compared to that of the free water. It is

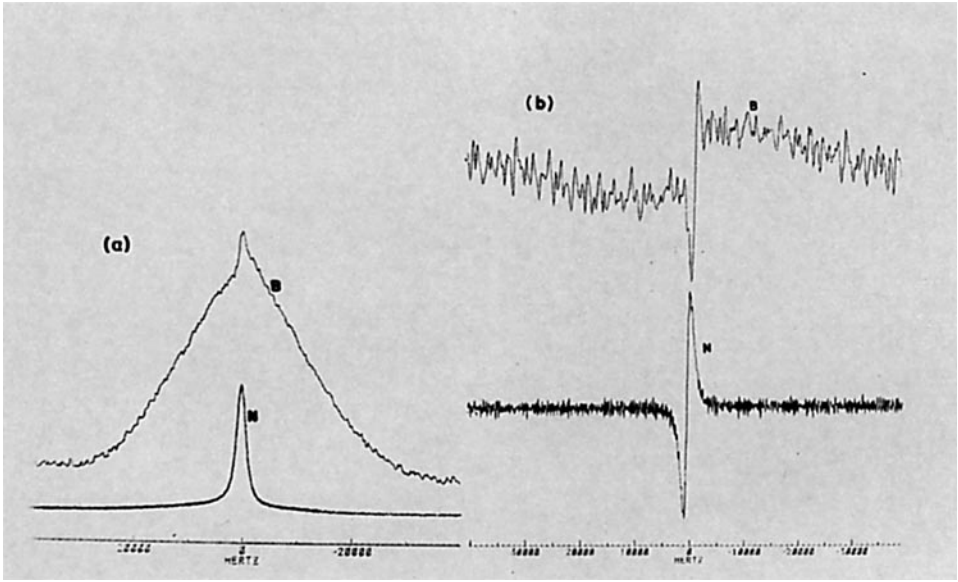

Figure 1 (a) NMR absorption and (b) derivative curves for Chokla wool equilibrated at 10.3% moisture regain; composite curve showing intense narrow component (N) and the weak broad component (B) is amplified for clarity.

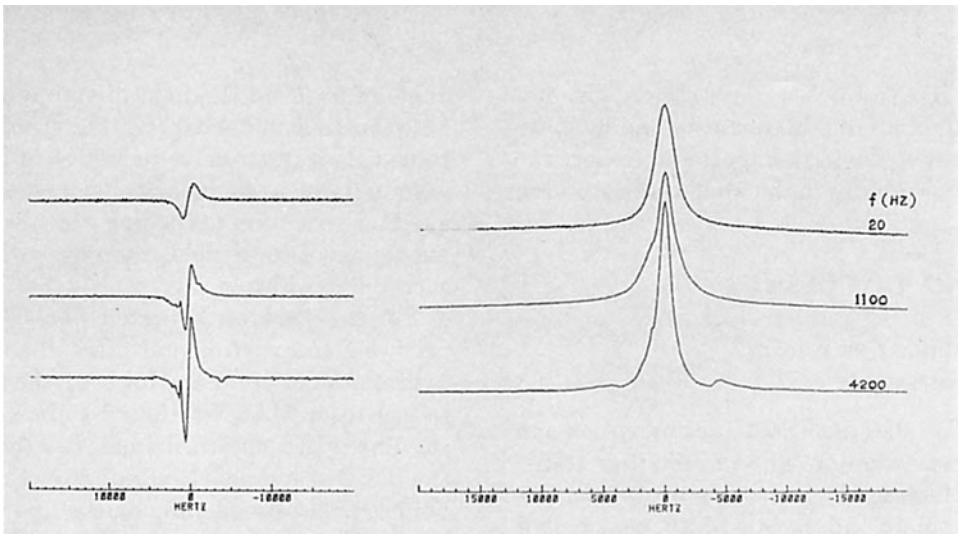

(a) (b)

Figure 2 NMR resonance lines for Chokla wool at 10.3% moisture regain spun at indicated frequencies (using MAS except for the low frequency test at 20 rpm). (a) Absorption and (b) derivative curves.

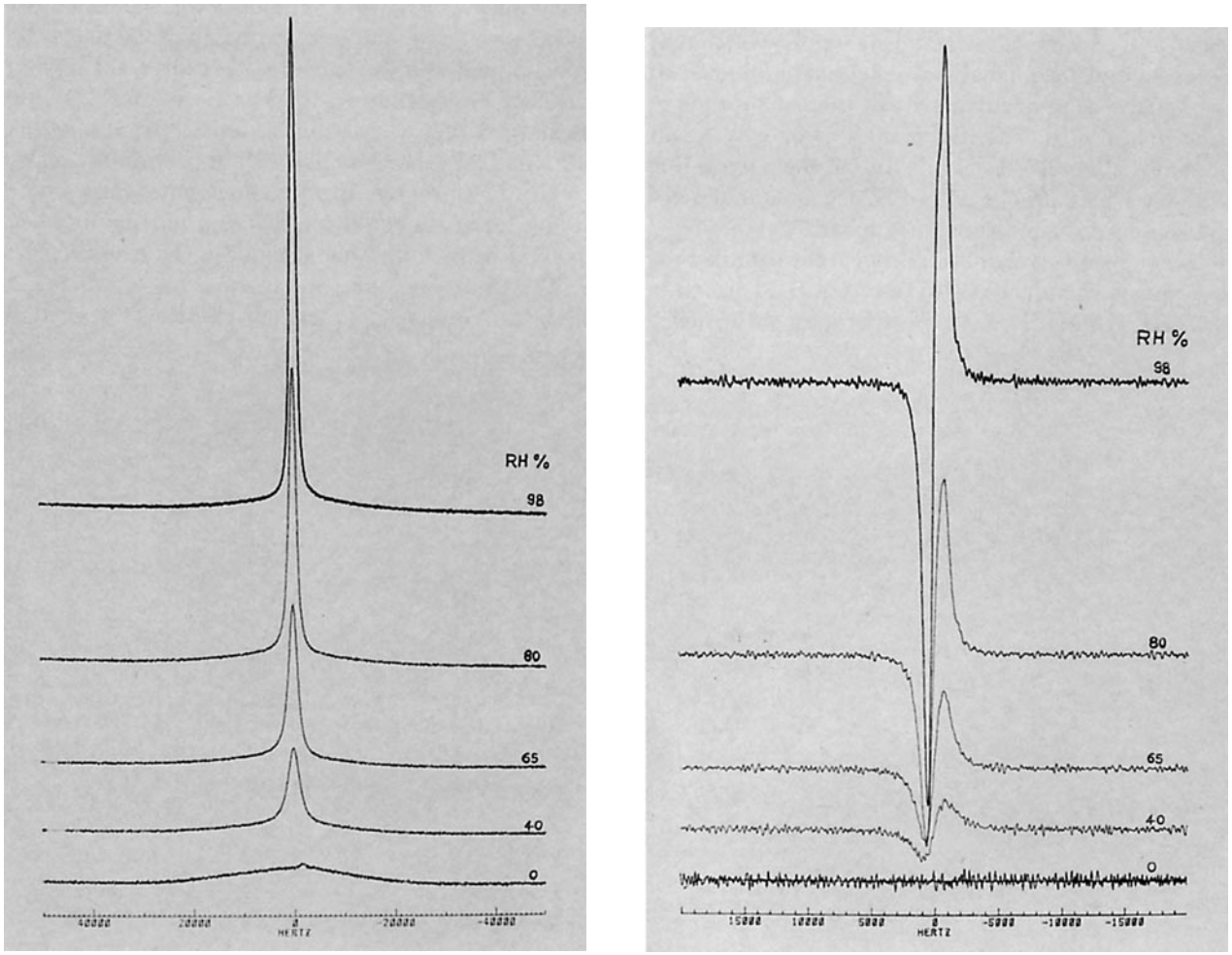

(a) (b)

Figure 3 (a) Absorption and (b) derivative curves of Chokla wool hydrated at indicated moisture regains.

interesting to note that starting with dry sample, which gives only the broad component, the samples with higher moisture contents give a proportionately more prominent narrow component. Since the broad component is not well-defined and also since our

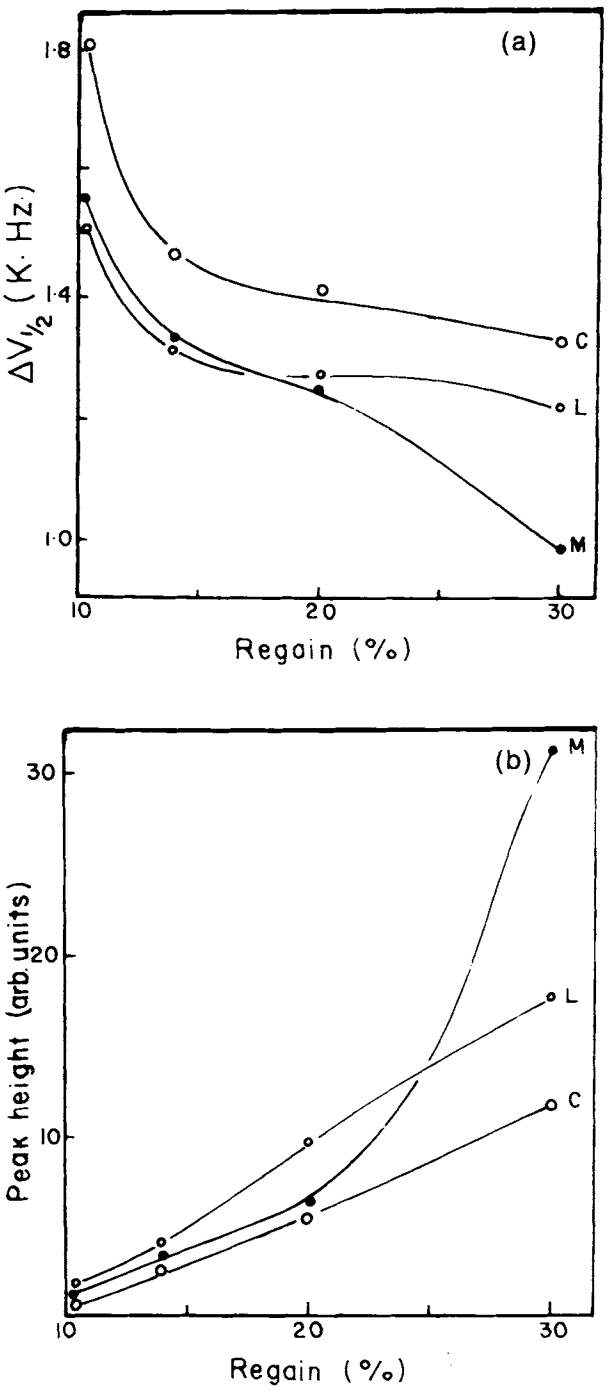

Figure 4 Effect of moisture content on NMR resonance curves. (a) Half-width and (b) peak height derived from derivative curves.

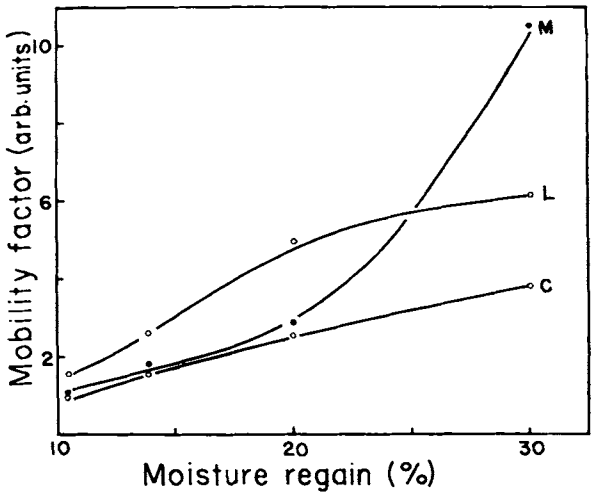

Figure 5 Mobility factor at various moisture regains.

main interest was in gaining an understanding of mobility, the analysis of the data will be restricted to the narrow component. The first derivative curves [Fig. 3(b)] clearly show progressive decrease in half-width with increase in moisture content. It was possible to obtain half-width and peak height from the digitized data of the Fourier transform spectrum, and the half-width and peak height results are shown in Figure 4(a) and 4(b), respectively. As already stated, line width relates to molecular motion; thus samples with higher moisture content have greater mobility. It is noteworthy that among the three wools studied Chokla shows [Fig. 4(a)] the highest half-width or lowest mobility at all moisture contents while Merino wool shows the highest mobility at higher regains. The peak height of the absorption curves is related to both the quality and mobility of water protons. It would appear from Figure 4(b) that the mobility is not very different for the three wools at low regains. Merino wool has relatively more mobility at higher regains compared to the other two wools.

It is noteworthy that the dependence of mobility on moisture regain in Lincoln and Chokla wools, as obtained in the present study, is in substantial agreement with the data on Corriedale wool reported by West et al.[9] However, the dependence of mobility on moisture regain is different in Merino wool, and this will be discussed later.

The mobility factor was calculated using the procedure outlined earlier, and the result is shown in Figure 5. Recalling that line width is inversely related to mobility, the similarity between the data shown in Figures 4(a) and 5, particularly at high regains, is not surprising. Similarity of the mobility

factor (Fig. 5) data to the peak height data [Fig. 4(b)] may also be noted, but this apparently arises because of the definition of mobility factor, which is directly related to peak height.

Relaxation Times

The spin–spin relaxation times (T_2) for the three wools were obtained from the magnetization decay curves. One such set of curves for Chokla wool sample at five hydration levels is shown in Figure 6. As stated earlier, the slope of the curve at a particular hydration gives T_2 for that sample. The decay curves show two main components. The keratin protons represent the fast decaying component (up to 10–20 μs), while the absorbed water protons form the slow decaying component (say above 50 μs). The slopes were therefore obtained for the solid lines of Figure 6, which relate to mobile water protons. The data for the other two wools were also similar. The T_2 data obtained by this method are shown in Figure 7(a). Since T_2 as measured represents the characteristic relaxation time of spin–spin interaction in the mobile phase, the similarity between the T_2 data [Fig. 7(a)] and the mobility factor (Fig. 5) on the one hand and between $1/T_2$ and half-width [Fig. 4(a)] on the other hand are not surprising.

The results of Lynch and Marsden[4] also show a reduction of T_2 with increase in regain, but the shape of the curves in the two cases are considerably different. However, it may be emphasized that in the present study, the T_2 relaxation curves are in good agreement with the half-width and other data. Thus the differences noted were possibly due to the differences in the experimental conditions.

The spin–lattice relaxation time, T_1, was obtained by the method described earlier, and the T_1 regain data are presented in Figure 7(b). T_1 values, as expected, are quite long because of the weak interactions between the spin system and the lattice. The T_1 data does not show a minimum (transition) with increasing moisture content, as predicted by theory.[3] This is apparently because of the high frequency of measurement and the lack of well-defined transitions in wool fiber.

Among the three wools studied, Merino wool shows the lowest T_1 at all moisture contents, indicating that relatively higher energy flow rate occurs in this fiber. Such a high rate is possibly facilitated by enhanced mobility of the molecular chains in the matrix, i.e., the spin energy of rigid chains in ordered fibril regions is propagated to mobile chains in the matrix that are capable of relaxing via the spin–lattice mechanism.

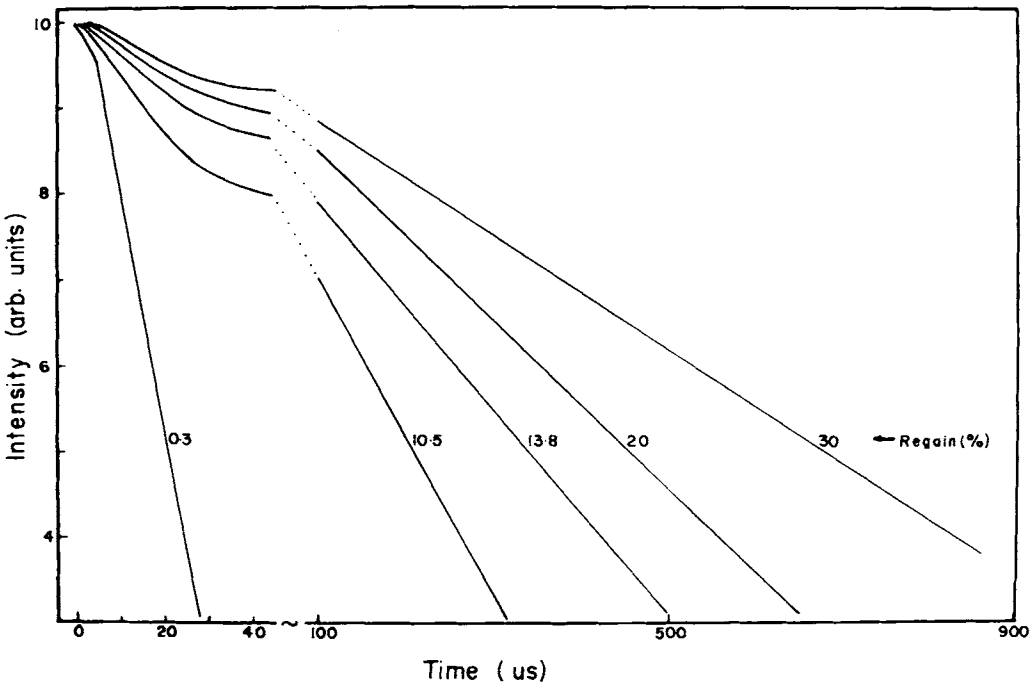

Figure 6 Magnetization decay curves for Chokla wool at different moisture regains (indicated).

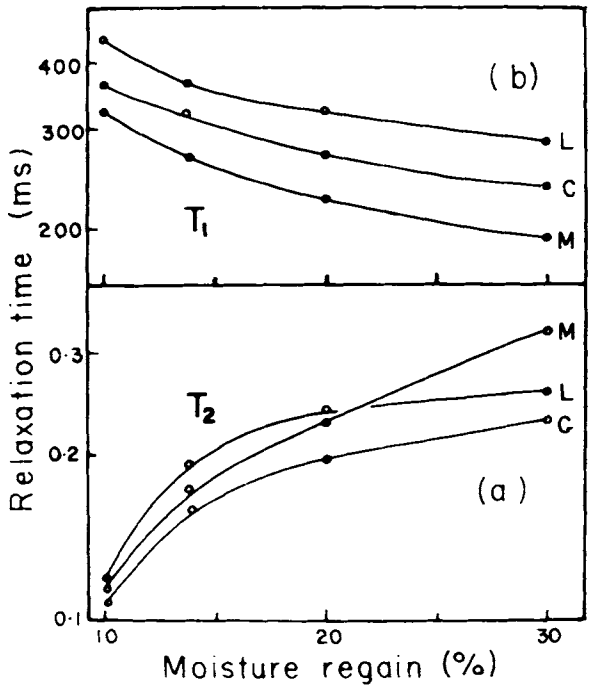

Figure 7 Variation of relaxation times with moisture regain. (a) Spin–spin relaxation time (T_2) and (b) spin–lattice relaxation time (T_1).

Mechanism of Water Sorption in Wool

For the wool–water system Figure 6 clearly shows the multicomponent nature of the decay signal. The absorbed water has been thought to exist in keratin in free and bound forms by Cassie;[15] in free, intermediate, and bound forms by Windle;[16] and in five different associations based on probability of having 0, 1, 2, 3, and 4 associations of hydrogen bonding to keratin molecules by Feughelman and Haly.[11] The Feughelman and Haly model, when simplified to two associations, closely agrees with Cassie's model. The present data was analyzed using these two models as they provide functional relation between regain and mass fraction of the water components. The Feughelman and Haly model gives justification on the basis of energy states of water–keratin hydrogen bonds; in the analysis using their model, the water molecules have been classified as follows:

1. Five components as originally given by Feughelman and Haly, viz. b_0, b_1, b_2, b_3, and b_4 representing zero, one, two, three, and four associations of hydrogen bonding between water and keratin, respectively. That is, b_0 corresponds to free water, the most mobile fraction, and b_4 corresponds to tightly bound water, the least mobile fraction.
2. Three components: b_0 (free), b_1 (intermediate), and b_2 (bound).
3. Two components: b_0 (free) and b_1 (bound).

Since each water fraction, having n components, is assumed to have a characteristic relaxation rate (R_n), the observed decay rate ($1/T_2$) can be related to R_n by the following equation[4]:

$$\frac{1}{T_2} = \sum_n P_n R_n \qquad (2)$$

where P_n is the probability of finding nuclear spin in the group whose relaxation rate is R_n. Using P_n values from Ref. 11 and assuming relaxation rate of the most mobile water component (b_0) equal to that of the liquid water, i.e., 0.286 s^{-1}, the experimental data on the three wools was analyzed to predict the relaxation rates of other water fractions. The best fit to the experimental data was obtained by the least-square minimization techniques using a computer and further by subjecting the data to the constraint that $R_n+1 > R_n$, i.e., the relaxation rate is higher for a water fraction having a higher number of associations, which implies that the most tightly bound fraction will have the highest relaxation rate.

The predicted relaxation rates are comparable in the three wool samples. This is interesting since the T_2 regain curves show significant differences in the three wools. The relaxation rates for Chokla wool are given in Table I, and the predicted $1/T_2$ curves are presented in Figure 8. The Feughelman and Haly model gives better fit than Cassie's model for any value of n. The fit between the calculated and the experimental data improves with increasing values of n and the best fit is thus found for $n = 5$.

Table I Relaxation Rate (R_n, s^{-1}) as a Function of Number of Keratin–Water Components (n)[a]

	Relaxation Rate ($\times 10^4$ s^{-1})		
Water Fraction	$n = 2$	$n = 3$	$n = 5$
b_1	0.91	0.65	0.61
b_2		2.80	1.09
b_3			1.70
b_4			1.81

[a] Rate for b_0 is 0.286 s^{-1}.

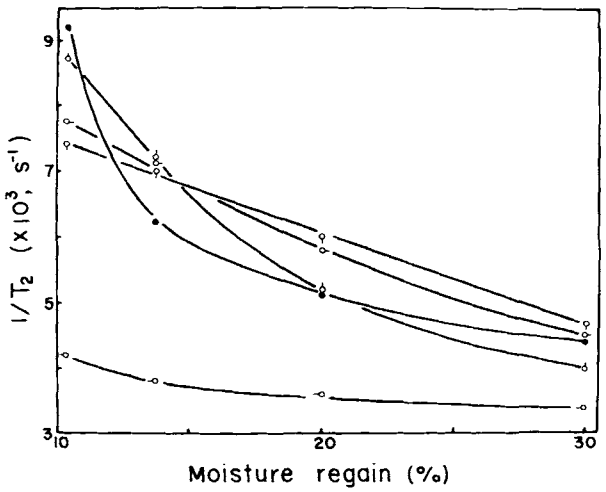

Figure 8 Comparison of the experimental and predicted values of I/T_2 from Eq. (2) for wool–water associations as follows: (●) experimental, (○) for Cassie's model; (–○), (○), (○–), and (○), for Feughelman and Haly's model for wool–water associations of 2, 3, and 5, respectively.

The significant observation of the present analysis is that the relaxation rates of bound water fractions are much different than those of the free water (by about 4 orders). Among the bound water fractions the relaxation rates vary little, and the maximum change is usually less than by a factor 2. These observations establish that free water fraction is different to others, and splitting bound water fractions beyond two gives better fit to the experimental data. As pointed out by Lynch and Marsden,[4] the relation between bound water fractions and moisture content predicted by the Feughelman and Haly model enables a close fit to the experimental data.

Studies on "Melted" Fibers

Wool fibers exhibit complete melting when subjected to water treatment at 135°C in the free condition or to water treatment at a slightly lower temperature, say 125°C, in the stretched condition.[17] Samples of "melted" fibers were prepared from the three wools in the above manner and studied. The half-width of the narrow line and the relaxation time data for three samples along with the corresponding data for the control sample are shown in Table II. It is interesting to note that on melting, the half-width shows an increase in both cases, while the relaxation times decrease compared to those of the control sample.

The spin–spin relaxation time has been shown to be related to the inverse of half-width. Thus the increase of half-width of the narrow line and decrease of T_2 in these samples suggest that in melted fibers the water protons have lower mobility. It was also observed that the peak intensity decreases in melted fibers. For example, in Lincoln wool, the peak intensity decreases to half or less than half its value for the control sample when the fiber is melted either in free or in stretched condition. The lower mobility of the water protons in the melted fibers may arise from the structural changes that take place in the control sample, which contains oriented α helices with some local order in the amorphous matrix. On melting, the helices transform to disoriented β form and the local order in the matrix disappears. This structural transformation results in the breakage of bonds between the side groups of α helices and the matrix. It is likely that some water molecules, which are present in free state in the control sample, can now become bound. As a result, the mobility of water protons will register a decrease as observed.

The decrease of spin–lattice relaxation time, T_1, on the other hand, relates to segmental mobility, as stated earlier. Svanson[8] has pointed out that, in primary absorption sites, water is assumed to be partly attached to hydrophilic groups of the polymer material and partly as a condensed phase that is in equilibrium with its surroundings. He further assumed that the water in primary position contributes

Table II NMR Parameters of Lincoln (L), Chokla (C), and Merino (M) Wool Samples Equilibrated at 40% RH

Extn. (%)	Temp. (°C)	Half-width (Hz)			T_2 (μs)			T_1 (ms)		
		L	C	M	L	C	M	L	C	M
Control		1320	1500	1350	190	160	166	433	361	318
0	135	1510	1550	1510	140	150	152	332	332	312
40	125	1580	1580	1600	153	116	136	288	281	274

to the broad line, while the more mobile secondary water in the condensed phase contributes to the narrow line. On hydration, the number of protons in the primary sites increase at the expense of the protons from the polymer chains. Thus, since segmental mobility would be expected to increase with increased regain, the decreased signal contribution from the protons of the polymer segments, which should occur with increased regain, should be compensated by a signal contribution arising from the protons of the primary absorbed water. The increased mobility of water in the primary sites during humidification can possibly be due to an increased segmental mobility because of the close and direct bonding between the water and the respective segments in the fiber. This enhanced segmental mobility then results in a decrease of T_1. The increased segmental mobility in the case of melted fibers as compared to the control fiber apparently arises as a result of structural changes on melting, e.g., bond breakage between the fibrils and the matrix, transformation from α to β form, and consequent disorientation and lack of order that follow melting.

Comparison between the Three Wools

The present studies have brought out some important differences between the three wools and these will be highlighted here.

First, there is a clear indication from the spin–lattice relaxation time (T_1) data [Fig. 7(b)] that the segmental mobility is highest in Merino wool, and this high segmental mobility is exhibited at all regains.

Second, the spin–spin relaxation time (T_2) data [Fig. 7(a)] and half-width of narrow line data [Fig. 4(a)] indicate that the water protons have higher mobility in Merino sample at high regains.

These differences could arise from the structural and morphological differences among the three wools. Merino fibers show bilateral structure, i.e., ortho- and para-type cells in near 2 : 1 proportion whereas the other two wools are predominantly para type.[17] Since ortho cells are known to show relatively poor microfibrillar packing[18] and higher proportion of bulky side groups,[19] ortho-rich Merino fibers will be expected to show low molecular orientation compared to the other two wools, as is found to be the case (Table III). Further, this agrees with the other structure–property relationships observed for these three wools.[17,20] The crystalline content, crystallite orientation, birefringence, and Young's modulus are the lowest in Merino wool, which also shows pronounced viscoelastic effects in creep and stress relaxation.

Table III Some Structural and Mechanical Properties of Wool Fibers at 25°C and 40% RH

Wool Type	Crystallinity (%)	Relative Crystallite Orientation	Birefringence	Young's Modulus (GPa)
Lincoln	30	0.82	0.0115	4.9
Chokla	27	0.81	0.0111	4.3
Merino	22	0.77	0.0094	3.4

Keeping these points in mind, the high mobility in Merino wool in the wet state can be explained along the following lines. In the dry state the matrix is glassy due to good molecular bonding, and the intermolecular bonding has an overwhelming effect on the molecular mobility, and the measured mobility reflects this. With the ingress of moisture the secondary bonds break and crosslink density, and the bulky groups becomes an important consideration. These were rigid in the dry state and can now generate more free volume and thus enhance the freedom of motion. The higher accessibility of the ortho regions in the wet state has been well established.[21] Thus, Merino wool, which has more accessible matrix compared to the other two wools and the relatively more uniform distribution of water in the matrix, would result in greater mobility at higher regains.

The authors are indebted to Dr. S. Ganapathy, National Chemical Laboratory, Pune, and his associate Dr. Rajamohanan for the assistance rendered in carrying out these experiments and for making useful comments on the manuscript. They are also grateful to the Director of NCL for permission to use the NMR facility. One of us (D. R. R.) wishes to acknowledge the support of the Indian Council of Agricultural Research, New Delhi, for the work reported in this and to Dr. N. B. Patil, Director, Cotton Technological research laboratory, Bombay, for permission to publish this paper.

REFERENCES

1. P. Hedvig, *J. of Polym. Sci., Macromol. Rev.*, **5**, 375 (1980).
2. J. H. Bradbury, W. F. Forbes, J. D. Leeder, and G. W. West, *J. Polym. Sci.*, **A2**, 3191 (1964).
3. J. Clifford and B. Sherard, *Biopolymers*, **4**, 1057 (1966).

4. L. Y. Lynch and K. H. Marsden, *J. Text. Inst.*, **57,** T1 (1966).
5. M. Miyagawa, K. Kohata, A. Takaka, and H. Kawai, *Sen-i Gakkaishi,* **43,** 57 (1987).
6. T. M. Shaw, R. H. Elsken, and R. E. Lundin, *J. Text. Inst.,* **51,** T562 (1960).
7. R. Shishoo and M. Lundell, *Text. Res. J.,* **42,** 285 (1972).
8. S. E. Svanson, *J. App. Polym. Sci.,* **22,** 571 (1978).
9. G. W. West, A. R. Haly, and M. Feughelman, *Text. Res. J.,* **31,** 899 (1961).
10. H. G. Olf and A. Peterlin, *J. Polym. Sci.,* **A2**(9), 2033 (1971).
11. M. Feughelman and A. R. Haly, *Text. Res. J.,* **32,** 966 (1962).
12. R. C. Weast, Ed., *CRC Hand Book of Chemistry and Physics,* 49th edition, E-37. The Chemical Rubber Co., Ohio, 1969.
13. G. C. Levy and I. R. Peat, *J. Magn. Reson.,* **18,** 500 (1975).
14. I. J. Lowe, *Phys. Rev. Lett.,* **2,** 285 (1959).
15. A. B. D. Cassie, *Trans. Faraday Soc.,* **41,** 458 (1945).
16. J. J. Windle, *J. Polym. Sci.,* **21,** 103 (1956).
17. D. Rama Rao, Structure Property Correlations in Some Wool Fibers, Ph.D. Thesis, Indian Institute of Technology, Delhi, 1989.
18. M. G. Dobb, *J. Text. Inst.,* **61,** T232 (1970).
19. P. L. Le Roux and J. B. Speakman, *Text. Res. J.,* **27,** 1 (1957).
20. V. B. Gupta and D. Rama Rao, *Text Res. J.,* to appear.
21. V. G. Kulkarni, R. M. Robson, and A. Robson, *Appl. Polym. Symposia,* **18,** 127 (1971).

Received March 21, 1991
Accepted April 17, 1991